Cosmology with low-redshift observations: No signal for new physics

Koushik Dutta,[1,*] Anirban Roy,[2,†] Ruchika,[3,‡] Anjan A. Sen,[3,§] and M. M. Sheikh-Jabbari [4,5,‖]

[1]*Theory Division, Saha Institute of Nuclear Physics, HBNI, 1/AF Salt Lake, Kolkata-700064, India*
[2]*SISSA, Via Bonomea 265, 34136 Trieste, Italy*
[3]*Centre for Theoretical Physics, Jamia Millia Islamia, New Delhi-110025, India*
[4]*School of physics, Inst. for research in fundamental sciences (IPM), P.O.Box 19395-5531 Tehran, Iran*
[5]*The Abdus Salam ICTP, Strada Costiera 11, 34151 Trieste, Italy*

We analyze various low-redshift cosmological data from Type-Ia supernova, baryon acoustic oscillations, time-delay measurements using strong-lensing, $H(z)$ measurements using cosmic chronometers and growth measurements from large scale structure observations for ΛCDM and some different dark energy models. By calculating the Bayesian evidence for different dark energy models, we find out that the ΛCDM still gives the best fit to the data with $H_0 = 70.3^{+1.36}_{-1.35}$ Km/s/Mpc (at 1σ). This value is in $\lesssim 2\sigma$ tension with various low and high redshift measurements for H_0 including SH0ES, Planck-2018 and the recent results from H0LiCOW-XIII. The derived constraint on $S_8 = \sigma_8 \sqrt{\Omega_{m0}/0.3}$ from our analysis is $S_8 = 0.76^{+0.03}_{-0.03}$, fully consistent with direct measurement of S_8 by KiDS + VIKING − 450 + DES1 survey. We hence conclude that the ΛCDM model with parameter constraints obtained in this work is consistent with different early and late Universe observations within 2σ. We therefore, do not find any compelling reason to go beyond concordance ΛCDM model.

I. INTRODUCTION

Different cosmological observations of the last couple of decades have surprised us with extraordinary results and puzzles, in particular the fact that our universe is now in an accelerated expansion, first confirmed by Type-Ia supernova observations (SN) [1,2] and later verified by host of other cosmological observations including the CMB [3,4] and LSS observations [5]. The evidence for the accelerated expansion requires existence of a repulsive gravity at large cosmological scales defying our usual notion of gravity as an attractive force. This demands either the existence of mysterious dark energy in the energy budget of the universe or the modification of Einstein gravity at large cosmological scales. A positive cosmological constant (Λ) is the simplest way to incorporate repulsive gravity in Einstein's GR. The concordance ΛCDM model is consistent with most of the cosmological observations today including the latest Planck-2018 [6] measurements of the cosmic microwave background (CMB). Nonetheless, cosmological constant as dark energy suffers from severe technical naturalness and from fine-tuning of the observed value

of Λ, motivating people to consider dark energy models beyond the cosmological constant.

The first serious tension for ΛCDM model emerges from the Local measurement of the expansion rate of the universe (SH0ES project) by Riess *et al.* in 2016 (R16) [7] and then the latest one in 2019 (R19) [8]. Their model independent measurement of the Hubble parameter at present is $H_0 = 74.03 \pm 1.42$ Km/s/Mpc which is in 4.4σ tension with the result $H_0 = 67.4 \pm 0.5$ Km/s/Mpc from the latest Planck-2018 [6] compilation for a concordance ΛCDM model. If one also combines the latest strong-lensing time-delay measurements of H_0 by H0LiCOW (H0LiCOW-XIII) [9] to the local measurement of H_0 by R19, the tension with Planck-2018 value of H_0 exceeds 5σ level for the ΛCDM model [10].

The effects of accelerated expansion and dark energy are also imprinted in the baryon acoustic oscillations (BAO) at the time of recombination. The observations of BAO peaks in galaxy surveys give accurate measurements of $r_d H_0$, the product of sound horizon size at drag epoch r_d and the present day Hubble parameter H_0. For the concordance ΛCDM model, CMB measurement by Planck-2018 gives $r_d = 147.05 \pm 0.30$ Mpc [6]. Using this value of r_d, inverse distance ladder method [11] using BAO and CMB, gives H_0 around 67 Km/s/Mpc, which is in more than 4σ tension with R19. On the other hand, assuming low-redshift anchor for H_0 from R16 and H0LiCow, BAO measurements gives r_d around 136 Mpc [12] irrespective of

*[*]koushik.physics@gmail.com
[†]aroy@sissa.it
[‡]ruchika@ctp-jamia.res.in
[§]aasen@jmi.ac.in
[‖]jabbari@theory.ipm.ac.ir

the dark energy model. This is in 3σ tension with value obtained by Planck-2018 for ΛCDM. While the amount of tension depends on how one calibrates BAO measurements, there is always a large tension between high and low redshift observations either for H_0 or for r_d.

This large tension may be due to unaccounted systematic in the local H_0 measurements. Whether we are living in a local underdense region or a void as possible systematic has been studied [13,14] (see however [15]), showing that this effect is too small to resolve the discrepancy of 6 Km/s/Mpc in H_0 between low and high redshift measurements [16]. Similarly, weak lensing of the supernova magnitudes has been shown to have too little effect to account for the current tension [17].

Efforts have also been made to introduce new physics both at early time as well as at late times to resolve this tension. Models with early dark energy [18], extra relativistic species [19], decay of dark matter to dark radiation [20,21], evolving dark energy [22–26], interacting dark energy [27], possibility of existence of negative cosmological constant [28,29], phantom dark energy [30], effect of non-Gaussian primordial fluctuation [31], existence of screened fifth force in the local universe [32], or modified gravity theory at low redshifts [33] are some of the recent attempts to resolve this tension.

Recently an independent local measurement of the H_0 has been carried out by the Carnegie-Chicago Hubble Program (CCHP) and presented by Freedman et al. (F19) [34]. Instead of the calibration using the Cepheids to Type-Ia supernova magnitudes, as used in R19 measurements, they have used the calibration of the tip of the red giant branch (TRGB) in the nearby galaxies. With this, F19 presented the measured local H_0 value which is $H_0 = 69.8 \pm 0.8$ (stat) ± 1.7(sys) Km/s/Mpc. This agrees with the Planck-2018 measured value within 1.2σ and with R19 measured value within 1.7σ. Given that the method of calibration in R19 and F19 are completely independent, the comparatively lower value obtained by F19 shows that one needs to be careful before drawing any conclusion on the tension between local measurement of H_0 and that extracted from the CMB. Recently, using both TRGB and SNe Ia distance ladder, Yaun et al. have determined the value for the Hubble constant to be $H_0 = 72.4 \pm 1.9$ Km/S/Mpc [35].

As mentioned above, the recent results by H0LiCOW-XIII [9] experiment for time-delay measurements with six strong lensing systems, have reported an independent measurement of H_0 for ΛCDM model which is $H_0 = 73.3^{+1.7}_{-1.8}$ Km/s/Mpc. This value is consistent with both R19 and F19 results but is in 3.1σ tension with Planck-2018 measured value. However, the measured values of H_0 for individual six lenses vary from 68.9 Km/s/Mpc to 81.1 Km/s/Mpc, too wide for any definite conclusion regarding the H_0 tension.

With this background, we reanalyze the available low-redshift observational data assuming different dark energy models which affects only the late time cosmology. We exclude the local measurements of H_0 either by R19 or F19 so that the measured values of different cosmological parameters including H_0, are not biased due to different calibrations used in R19 and F19. While using the BAO data, we also do not bias our results by assuming a prior on r_d (sound horizon scale at drag epoch) as given by Planck-2018. We allow it to be a free parameter in our analysis and determine it from low-redshift observations to corroborate with the findings from the Planck-2018 results. Our aim is to examine if low-redshift data (without local measurement of H_0) also exhibit significant tensions in measured values of different cosmological parameters. In the next two sections we respectively discuss the dark energy models/ parametrizations and cosmological data that we use for our analysis. We then present our results. Finally, we conclude with some discussions that includes the implications of our results for S_8 observations.

II. MODELING LATE TIME COSMOLOGY

To begin with, we assume spatially flat FRW cosmology for the background universe and normalise the present value of scale factor $a_0 = 1$. Throughout the manuscript, subscript "0" represents parameter values at present ($z = 0$). We consider the following dark energy models for our background cosmology:

(i) ΛCDM model with the Hubble parameter $H(z)$,

$$\frac{H^2(z)}{H_0^2} = \Omega_{m0}(1 + z)^3 + (1 - \Omega_{m0}). \quad (1)$$

Here Ω_{m0} is matter density parameter today.

(ii) wCDM model with dark energy model of a constant equation of state w and the Hubble parameter $H(z)$,

$$\frac{H^2(z)}{H_0^2} = \Omega_{m0}(1 + z)^3 + (1 - \Omega_{m0})(1 + z)^{3(1+w)}.$$

$$(2)$$

(iii) CPL model: Dark energy model with an equation of state $w(z) = w_0 + w_a(1 - a) = w_0 + w_a \frac{z}{1+z}$ where w_0 and w_a are two arbitrary constants [36,37] and

$$\frac{H^2(z)}{H_0^2} = \Omega_{m0}(1 + z)^3 + (1 - \Omega_{m0})f(z), \quad (3)$$

where $f(z) = \exp\left(3\int^z \frac{(1+w(x))}{1+x}dx\right)$.

(iv) Pade model for dark energy: Unlike the previous cases we do not assume any specific parametrization for the dark energy equation of state. Rather, we assume a generic dark energy behavior beyond a cosmological constant Λ. The simplest way to model deviation from a constant dark energy density is Taylor-expansion around Λ for the dark energy

density. As we are interested in the low-redshift observations, we do the expansion around the present day ($a_0 = 1$):

$$\rho_{de}(a) = \rho_0 + \rho_1(1 - a) + \rho_2(1 - a)^2 + \cdots \quad (4)$$

Here ρ_0 is the present value of the dark energy density and ρ_1 and ρ_2 are two expansion parameters. If one rewrites the above expression in terms of the redshift z, the dark energy density takes the form:

$$\rho_{de}(a) = \frac{\rho_0 + (2\rho_0 + \rho_1)z + (\rho_2 + \rho_1 + \rho_0)z^2}{1 + 2z + z^2}$$

which is Pade expansion of order (2,2) around $z = 0$ with properly identified expansion coefficients [38]. In our subsequent analysis, we assume the dark energy density as a general Pade expansion of order (2,2) around $z = 0$. The Hubble parameter $H(z)$ is then given by

$$\frac{H^2(z)}{H_0^2} = \Omega_{m0}(1 + z)^3 + (1 - \Omega_{m0})\mathcal{P}(z), \quad (5)$$

where

$$\mathcal{P}(z) = \frac{1 + P_1 z + P_2 z^2}{1 + Q_1 z + Q_2 z^2}, \quad (6)$$

with P_1, P_2, Q_1, and Q_2 being four expansion parameters. This parametrization of dark energy density allows a host of dark energy behavior including phantom to nonphantom crossing as well as a negative effective dark energy density which may arise in scalar tensor theory models of dark energy [28]. Note that for very small and very large redshifts, the dark energy density approaches a constant value as in cosmological constant and the model approaches ΛCDM.

III. DATASETS USED

To constrain different dark energy models mentioned above, we consider the following observational data:

(i) Isotropic BAO measurements by 6dF survey ($z = 0.106$) [39], SDSS-MGS survey ($z = 0.15$) [40] as well as by eBOSS quasar clustering ($z = 1.52$) [41]. We also consider anisotropic BAO measurements by BOSS-DR12 at $z = 0.38$, 0.51, 0.61 [42]. Finally we consider BAO measurement by BOSS-DR12 using Lyman-α samples at $z = 2.4$ [43]. Hereafter, we will call all these data together as "BAO" data.

(ii) Angular diameter distances measured using water megamasers under the Megamaser Cosmology Project at redshifts $z = 0.0116$, 0.0340, 0.0277 for

TABLE I. Parameters used in different models and their prior.

Parameter	Models	Prior (uniform)
Ω_{m0}	All	[0.1, 0.9]
H_0	All	[50, 90] Km/s/Mpc
σ_8	All	[0.6, 1.0]
r_d	All	[130,170]
w	wCDM,	[−1.9, −0.4]
w_0	CPL	[−1.9, −0.4]
w_a	CPL	[−4.0, 4.0]

Megamasers UGC 3789, NGC 6264 and NGC 5765b respectively [44–47], hereafter "MASERS". We will also make some comments on the very recent NGC 4258 data and its implications for H_0 [48] in the discussion part.

(iii) Strong lensing time-delay measurements by H0Li-COW experiment (TDSL) by Bonvin *et al.* (2017) [49] for three lens systems, hereafter "SL" data. Note that we have not considered the recent H0LiCOW-XIIIsurements [9] of six lenses. We discuss this in the latter part of the paper.

(iv) Latest Pantheon data for SNIa in terms of $H(z)/H_0$ as compiled by Gomez-Valent and Amendola (2018) [50], here- after "SN" data.

(v) OHD data for Hubble parameter as a function of redshift using cosmic chronometers as compiled in Gomez-Valent and Amendola (2018) [50], hereafter "CC" data.

(vi) Finally, the measurements of $f\sigma_8$ by various galaxy surveys as compiled by Nesseris *et al.* [51], hereafter "$f\sigma_8$" data. This is "Gold-17" sample for $f\sigma_8$ measurements. We have implemented the corrections for the dependence on fiducial cosmology used to convert redshifts into distances as described in [51] (see also [52]). Here f is the growth parameter for the linear matter density fluctuation $f = \frac{d\log\delta}{d\log a}$, with δ being the linear matter overdensity and σ_8 is the *rms* fluctuation of linear matter overdensity on $8h^{-1}$ Mpc scale.

Combination of the first four set of data (BAO + MASERS + SL + SN) is termed as "BASE" set in our subsequent analysis. The priors for different parameters considered in our analysis are given in Table I. We use the publicly available code "Emcee" [53] to generate the MCMC for different models for the above set of data.

IV. RESULTS

The constraints on different cosmological as well as model parameters for different combination of data, are shown in Tables II, III, IV, and V. Different columns in these tables correspond to different combinations of datasets where we separate out the effects of adding cosmic

TABLE II. Constraints on parameters for ΛCDM for different set of observation data. The error bars quoted are at 1σ confidence interval. "BASE" denotes "BAO + MASERS + SL + SN".

		ΛCDM	
Parameters	BASE	+CC	+$f\sigma_8$
Ω_{m0}	$0.29^{+0.014}_{-0.014}$	$0.29^{+0.013}_{-0.013}$	$0.29^{+0.013}_{-0.013}$
r_d (Mpc)	$141.72^{+4.55}_{-4.56}$	$144.66^{+2.81}_{-2.83}$	$144.71^{+2.9}_{-2.9}$
H_0 (Km/s/Mpc)	$71.74^{+2.22}_{-2.22}$	$70.26^{+1.38}_{-1.37}$	$70.3^{+1.36}_{-1.35}$
σ_8	—	—	$0.77^{+0.03}_{-0.03}$
$S_8 = \sigma_8\sqrt{\Omega_{m0}/0.3}$	—	—	$0.76^{+0.03}_{-0.03}$

TABLE III. The same as Table II but for wCDM model.

		wCDM	
Parameters	BASE	+CC	+$f\sigma_8$
Ω_{m0}	$0.284^{+0.018}_{-0.018}$	$0.285^{+0.017}_{-0.017}$	$0.30^{+0.009}_{-0.009}$
r_d (Mpc)	$141.76^{+4.44}_{-4.48}$	$144.77^{+2.88}_{-2.87}$	$144.51^{+2.90}_{-2.92}$
H_0 (Km/s/Mpc)	$71.44^{+2.21}_{-2.17}$	$69.97^{+1.4}_{-1.4}$	$70.27^{+1.44}_{-1.43}$
w	$-0.96^{+0.07}_{-0.06}$	$-0.96^{+0.06}_{-0.06}$	$-1.02^{+0.03}_{-0.03}$
σ_8	—	—	$0.76^{+0.03}_{-0.03}$
$S_8 = \sigma_8\sqrt{\Omega_{m0}/0.3}$	—	—	$0.756^{+0.03}_{-0.03}$

TABLE IV. The same as Table II but for CPL model.

		CPL	
Parameters	BASE	+CC	+$f\sigma_8$
Ω_{m0}	$0.232^{+0.054}_{-0.063}$	$0.23^{+0.054}_{-0.06}$	$0.241^{+0.039}_{-0.041}$
r_d (Mpc)	$141.28^{+4.56}_{-4.63}$	$144.75^{+2.8}_{-2.73}$	$144.88^{+2.84}_{-2.95}$
H_0 (Km/s/Mpc)	$71.87^{+2.33}_{-2.28}$	$70.22^{+1.4}_{-1.4}$	$70.19^{+1.48}_{-1.46}$
w_0	$-0.96^{+0.08}_{-0.08}$	$-0.96^{+0.08}_{-0.08}$	$-0.97^{+0.07}_{-0.07}$
w_a	$0.56^{+0.42}_{-0.46}$	$0.57^{+0.41}_{-0.45}$	$0.56^{+0.38}_{-0.39}$
σ_8	—	—	$0.85^{+0.08}_{-0.07}$
$S_8 = \sigma_8\sqrt{\Omega_{m0}/0.3}$	—	—	$0.76^{+0.029}_{-0.029}$

TABLE V. The same as Table II but for Pade model.

		PADE	
Parameters	BASE	+CC	+$f\sigma_8$
Ω_{m0}	$0.355^{+0.12}_{-0.12}$	$0.31^{+0.09}_{-0.07}$	$0.263^{+0.046}_{-0.044}$
r_d (Mpc)	$140.35^{+4.7}_{-4.81}$	$144.76^{+2.9}_{-2.9}$	$145.06^{+2.95}_{-2.94}$
H_0 (Km/s/Mpc)	$73.6^{+2.7}_{-2.7}$	$71.22^{+1.8}_{-1.8}$	$71.14^{+1.7}_{-1.7}$
P_1	$-0.735^{+2.31}_{-1.92}$	$1.48^{+2.28}_{-2.13}$	$2.55^{+1.58}_{-1.59}$
P_2	$-0.43^{+1.92}_{-1.83}$	$0.17^{+1.99}_{-1.65}$	$0.67^{+2.11}_{-2.05}$
Q_1	$0.9^{+1.98}_{-1.2}$	$1.49^{+2.16}_{-1.78}$	$2.41^{+1.69}_{-1.77}$
Q_2	$0.14^{+0.11}_{-0.11}$	$0.101^{+0.096}_{-0.098}$	$0.095^{0.09}_{-0.09}$
σ_8	—	—	$0.700^{+0.03}_{-0.03}$
$S_8 = \sigma_8\sqrt{\Omega_{m0}/0.3}$	—	—	$0.654^{+0.06}_{-0.06}$

chronometers (CC) data, and the $f\sigma_8$ data. As one can see from these tables, the constraints on three cosmological parameters (Ω_{m0}, r_d, H_0), are nearly the same for different dark energy models except that CPL and Pade prefer slightly lower value of Ω_{m0} and Pade prefers slightly higher value for H_0. But all of them are consistent within 1σ error bar. Note that the inclusion of cosmic chronometers data always makes the H_0 value smaller which is more compatible with the derived H_0 value from the high red-shift data. Further inclusion of $f\sigma_8$ does not change H_0 value much. All the values of H_0 for different dark energy models for the full datasets (BASE+CC+$f\sigma_8$) are fully consistent with F19 [34]. For ΛCDM, we obtain $H_0 = 70.3^{+1.36}_{-1.35}$ for full datasets. This is in tension with both Planck-2018 [6] and R19 [8] results at 2.01σ and 1.9σ respectively and with recent H0LiCOW-XIII measurements for six lenses at 1.33σ. In other words, for ΛCDM, our H_0 measurement with various low-redshift observations are consistent with R19, F19, Planck-2018 as well as recent H0LiCOW-XIII [9] measurements with 2σ or less error bar. Moreover, this result still holds for our different dark energy models. Note that we use the H0LiCOW(2017) data for three lenses, however, our measured value for H_0 is consistent with the combined measurement for H_0 by latest H0LiCOW-XIII for six lenses. Figure 1 depicts the marginalized H_0 value with 1-σ error for different models for different combinations of the data, clearly showing the consistency of H_0 measurements for different dark energy models.

At this point, it is important to remind ourselves that the derived parameter values must not be in substantial conflict with the high red-shift Planck data. In our analysis, we do not take the full Planck likelihood in consideration to derive
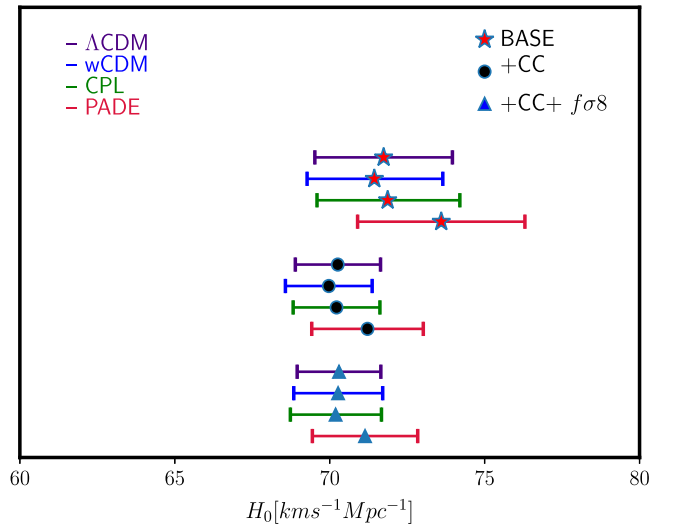

FIG. 1. Values of H_0 with 1-σ error for several models studied in the work. The results are shown for different combinations of datasets studied.
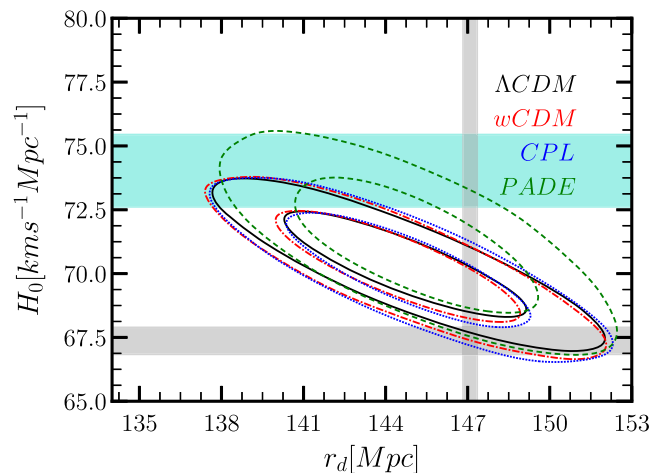
FIG. 2. 1σ and 2σ constrained contours in $H_0 - r_d$ parameter plane. The horizontal green band is 1σ constraints on H_0 by R19. The horizontal (vertical) grey band is constraint on H_0 (on r_d) from Planck-2018. Here the "BASE+CC+$f\sigma_8$" datasets is used.

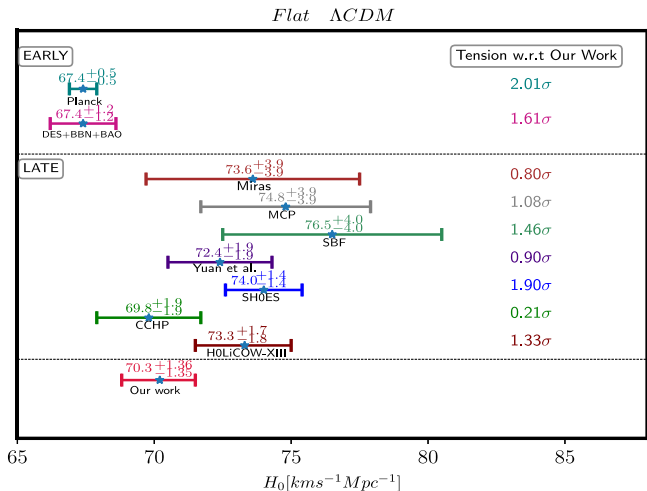

FIG. 3. H_0 measurements with 1σ error bars from different observational data including the one reported in this work for ΛCDM model. We also show the tensions in our measurement with low-redshift observations compared to other observations. The DES + BBN + BAO, MIRAS, MCP and SBF measurements are taken from [10]. For the rest of the measurements, see the text.

the best fit parameters. Rather, we cross-check that our derived parameters are not in major deviations from the Planck-2018 parameter values. As noted in the Introduction, CMB measurements by Planck-2018 gives the sound horizon scale at drag epoch $r_d = 147.05 \pm 0.30$ Mpc. Using the low red-shifts data, we obtain $r_d = 144.68^{+2.9}_{-2.9}$ for ΛCDM model with all the datasets, which is in less than 1σ tension with Planck-2018 result. Here also, note the importance of cosmic chronometers data whose inclusion always makes the r_d value larger, making it more consistent with CMB result for r_d.

In Fig. 2, we show the constraint in the (H_0, r_d) contour plane. As one can see, the constrained contours are very similar for different dark energy models and both H_0 and r_d constraints are consistent with R19 and also with the Planck-2018 measurements.

To summarize, the combination of "BASE + CC + $f\sigma_8$" gives consistent constraints on both H_0 and r_d parameters for different dark energy models showing no preference for models beyond ΛCDM. Moreover the constraints on $H_0 = 70.3^{+1.36}_{-1.35}$ for ΛCDM model is in 2σ or less tension with both high-redshift (Planck-2018, DES + BBN + BAO) and local measurements (R19, F19, H0LiCOW). This is depicted in Fig. 3 where different measurements for H_0 (as quoted in [10]) are shown including that from the current analysis. We also show the tension in our current H_0 measurement with other H_0 measurements; in all cases the tensions are within 2σ or less.

Finally we calculate the "Bayesian evidence" or "global likelihood" for the dark energy models considered in this work. The Bayesian evidence is defined as

$$\mathcal{Z} = \int P(D|\theta)P(\theta)d^w\theta. \qquad (7)$$

Here D represents the data considered, θ represent the model parameters, w is the dimension of the parameter space, $P(D|\theta)$ represents the likelihood function for the parameters θ given the data D and $P(\theta)$ is the prior distribution for the parameters θ. With this, we use the Jeffrey's scale for Bayesian evidence to compare models. In particular if $\Delta Ln\mathcal{Z}$ between two models is more than 2.5, then the model with higher $Ln\mathcal{Z}$ is strongly favored compared to the model with lower $Ln\mathcal{Z}$ and for $\Delta Ln\mathcal{Z} > 5$, it is decisively favored. In Table VI, we show the Bayesian evidence for different dark energy models: ΛCDM has the highest $Ln\mathcal{Z}$ compared to other dark energy models considered and is therefore still the best model for the low-redshift observational data "SN + BAO + MASERS + SL + CC + $f\sigma_8$". Interestingly, the wCDM is decisively ruled out compared to ΛCDM by the low-redshift data and both CPL and PADE are also strongly disfavored compared to ΛCDM. For completeness, we have also presented the χ^2 and $\chi^2/$d.o.f for each model in Table VI for comparison of the goodness of fit.

TABLE VI. χ^2 values and Bayesian Evidence for different dark energy models for all datasets. In the last row, we mention that difference of $Ln\mathcal{Z}$ from ΛCDM for three other models.

	ΛCDM	wCDM	CPL	PADE
χ^2	84.27	89.85	82.94	80.74
$\chi^2/$d.o.f	1.29	1.40	1.32	1.32
$Ln\mathcal{Z}$	-60.59	-69.08	-63.24	-63.38
$\Delta(Ln\mathcal{Z})$	$\cdots$	-8.49	-2.65	-2.79

V. DISCUSSION AND CONCLUSIONS

As discussed, BAO observations measure the combination $H_0 r_d$ rather than H_0 and r_d individually. In our analysis, we include the BAO measurement by BOSS-DR12 with Lyman-α samples at redshift $z = 2.4$. To see the effect of this particular observation from BAO-Lyman-α in our analysis, we show in Fig. 4, the constraints on the combination $H_0 r_d$ for different dark energy models with and without this Lyman-α measurement at $z = 2.4$. As one can see, the Lyman-α data for BAO at $z = 2.4$ does not affect the constraint on the combination $H_0 r_d$. Constraints on $H_0 r_d$ are uniform across different dark energy models considered in this analysis, except for the Pade which gives a slightly higher mean value, and our $H_0 r_d$ value is consistent with Planck-2018 within 2σ. There are updated results for BAO-Lyman-α measurement by eBOSS-DR1 [54] for which the tension with Planck-2018 has been reduced. However, from Fig. 2 we can safely conclude that incorporating this updated data will have minimal effect on our results.

Next, we explore another tension between the high-redshift CMB and the corresponding low-redshift measurements. This is related to the growth of large scale structures in the Universe. Weak lensing by large scale structures is one of the most accurate probes to measure the growth of structures in the Universe and the underlying cosmology. The Kilo-Degree Survey (KiDS) spanning 450 square-degrees in the sky combined with VISTA Kilo Degree Infra-Red Survey (VIKING) [55], has recently performed a robust tomographic cosmic shear analysis and measured the S_8 parameter related to the amplitude of the cosmic shear due to weak lensing: $S_8 = 0.737^{+0.040}_{-0.036}$. This measured value is in 2.3σ tension with the corresponding value obtained by Planck-2018 for ΛCDM. There is, moreover, a combined tomographic weak lensing
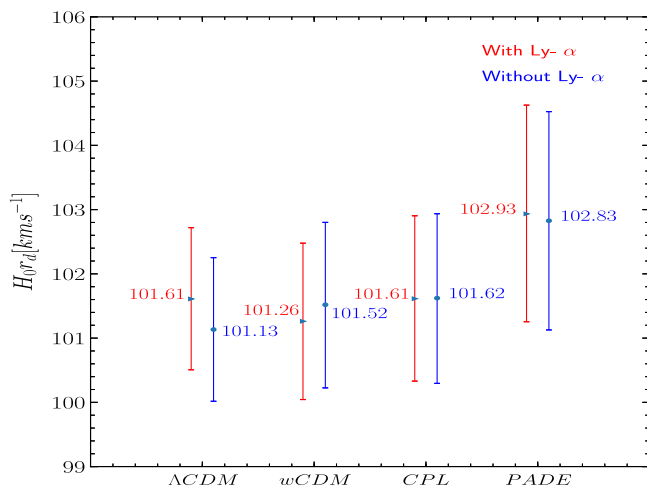
analysis of KiDS + VIKING and Dark Energy Survey (DES-Y1) [56]. The constraint on S_8 from this combined analysis is $S_8 = 0.762^{+0.025}_{-0.024}$ which is in 2.5σ tension with Planck-2018 result for ΛCDM. These tensions are not as large compared to H_0 tension discussed before and we still do not know whether this tension between early and late universe measurements is due to unknown systematic or it hints some new physics beyond ΛCDM model.

In our current analysis, however, we have obtained an independent constraint on S_8 solely from the low-redshift observations using measurements of $f\sigma_8$ by various surveys. Note that for ΛCDM model and assuming Einstein GR is the correct theory of gravity, $f\sigma_8 \sim \Omega_m^{0.55} \sigma_8$ whereas S_8 scales as $S_8 \sim \Omega_m^{0.5} \sigma_8$. Hence, if ΛCDM is the true model, using $f\sigma_8$ data itself, one also expects to get strong constraint on S_8. Moreover, if ΛCDM is a true model, from these two scaling relations, one expects a very small correlation between S_8 and Ω_{m0}.

For different dark energy models the constraint on S_8 are shown in Tables II, III, IV, and V. The constraint on S_8 is comparable for different dark energy models except for Pade where the mean value is substantially less, but with a larger error bar. In particular, the constraint is $S_8 = 0.76^{+0.03}_{-0.03}$ for ΛCDM which is perfectly consistent with KiDS + VIKING-450 + DES-Y1 result, though with slightly larger error bars compared to the latter. The confidence contours in (S_8, Ω_{m0}) and in (S_8, H_0) parameter space are shown in Fig. 5 which shows negligible correlation between S_8 and Ω_{m0} for wCDM and CPL models confirming no deviation from ΛCDM behavior. This confirms that the independent indirect measurement of S_8 using low-redshift "BASE + CC + $f\sigma_8$" dataset, is fully consistent with the direct measurement of S_8 by KiDS + VIKING-450 + DES-Y1. In this case, too, there is no need to go beyond ΛCDM.

To conclude, we revisit the low-redshift observational data "SN + BAO + MASERS + SL + CC + $f\sigma_8$" assuming different dark energy models including ΛCDM. Our goal is to check what the low-redshift data alone has to say about the current tension in H_0 measurements from early and late Universe. Our results show that the low-redshift datasets yield consistent constraints for cosmological parameters across different dark energy models and the constraints on H_0 and r_d are consistent with both R19 and Planck-2018 measurements to 2σ level. In drawing this conclusion, the addition of cosmic chronometers data $H(z)$ plays a crucial role by pushing H_0 value toward a smaller value (closer to the Planck results), whereas making r_d larger. Also our derived value of S_8 is fully consistent with the direct measurement of S_8 by KiDS + VIKING-450 + DES-Y1 survey. We show that there is no clear evidence for models beyond ΛCDM for this set of low-redshift data. Moreover in terms of Bayesian Evidence, ΛCDM is still the best model compared to other dark energy models analyzed. Just recently,

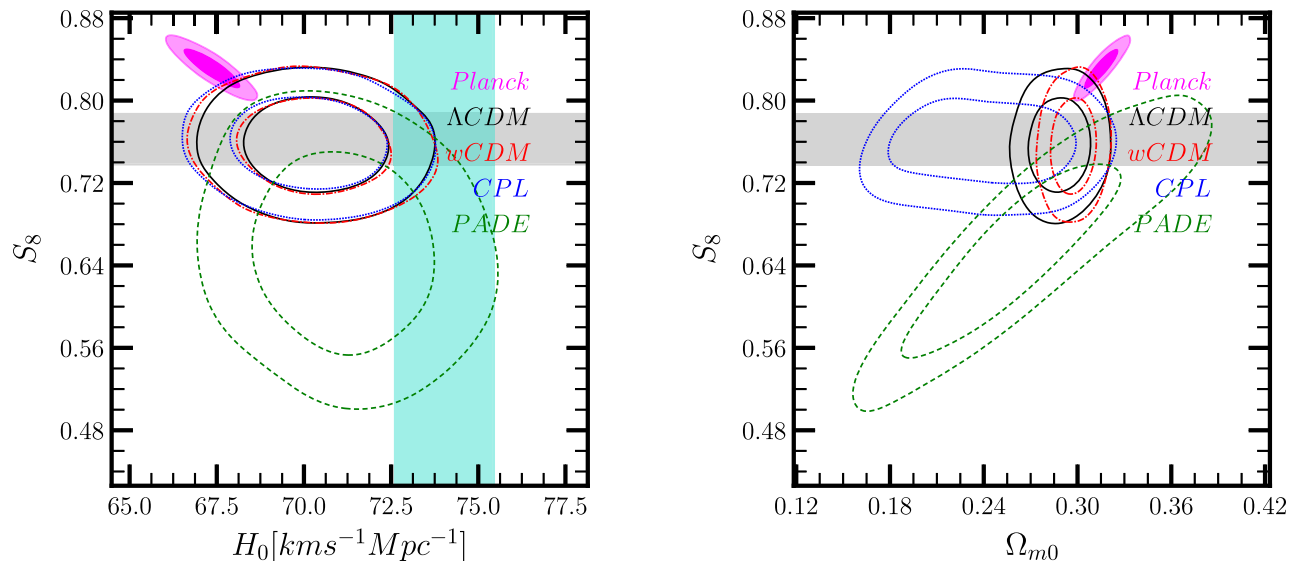FIG. 4. Values of $H_0 r_d$ (in Km/s) for different dark energy model. The dataset used "BASE + CC".

FIG. 5. 1σ and 2σ contours in (H_0, S_8) plane (left figure) and in (Ω_{m0}, S_8) (right figure) for different dark energy models. The grey band is 1σ bound for S_8 from KiDS + VIKING-450 + DES-Y1 survey results. The green band in the left figure is the 1σ bound on H_0 from R19.

a improved distance to megamaser NGC-4258 have been measured giving an updated estimate for H_0 which is $H_0 = 71.1 \pm 1.9$ KM/s/MPc [48]. This is fully consistent with our measured value of H_0 for ΛCDM as quoted in Table II with a tension less than 1σ. Moreover, Liao *et al.* have recently obtained a model independent H_0 constraint using the SnIa and strong lensing measurement by H0LiCOW. Their model independent constraint is $H_0 = 72.2 \pm 2.1$ KM/s/MPc [57] for a spatially flat Universe which is in less than 1σ tension with our result for ΛCDM confirming again the consistency of our result with other constraints obtained by different methods.

The ΛCDM with model parameters as shown in Table II is consistent with R19, F19, Planck-2018, H0LiCOW-XIII as well as KiDS + VIKING-450 + DES-Y1 and the tensions with each of these observations are always within 2σ or less. Hence ΛCDM model with parameters as mentioned

in Table II best represents the current Universe without any significant tension.

[1] S. Perlmutter *et al.* (Supernova Cosmology Project), Astrophys. J. **517**, 565 (1999).

[2] A. G. Riess *et al.* (Supernova Search Team), Astron. J. **116**, 1009 (1998).

[3] E. Komatsu *et al.* (WMAP Collaboration), Astrophys. J. Suppl. Ser. **192**, 18 (2011).

[4] P. A. R. Ade *et al.* (Planck Collaboration), Astron. Astrophys. **571**, A16 (2014).

[5] M. Tegmark *et al.* (SDSS Collaboration), Phys. Rev. D **69**, 103501 (2004).

[6] N. Aghanim *et al.* (Planck Collaboration), arXiv:1807.06209.

[7] A. G. Riess *et al.*, Astrophys. J. **826**, 56 (2016).

[8] A. G. Riess, S. Casertano, W. Yuan, L. M. Macri, and D. Scolnic, Astrophys. J. **876**, 85 (2019).

[9] K. C. Wong *et al.*, arXiv:1907.04869.

[10] L. Verde, T. Treu, and A. G. Riess, Nat. Astron. **3**, 891 (2019).

[11] E. Aubourg *et al.*, Phys. Rev. D **92**, 123516 (2015).

[12] J. Evslin, A. A. Sen, and Ruchika, Phys. Rev. D **97**, 103511 (2018).

[13] H.-Y. Wu and D. Huterer, Mon. Not. R. Astron. Soc. **471,** 4946 (2017).

[14] W. D. Kenworthy, D. Scolnic, and A. Riess, Astrophys. J. **875,** 145 (2019).

[15] E. O. Colgáin, J. Cosmol. Astropart. Phys. 09 (2019) 006.

[16] H. Boehringer, G. Chon, and C. A. Collins, arXiv:1907 .12402.

[17] M. Smith *et al.* (SDSS Collaboration), Astrophys. J. **780,** 24 (2014).

[18] V. Poulin, T. L. Smith, T. Karwal, and M. Kamionkowski, Phys. Rev. Lett. **122,** 221301 (2019).

[19] M. Wyman, D. H. Rudd, R. A. Vanderveld, and W. Hu, Phys. Rev. Lett. **112,** 051302 (2014).

[20] K. L. Pandey, T. Karwal, and S. Das, arXiv:1902.10636.

[21] K. Vattis, S. M. Koushiappas, and A. Loeb, Phys. Rev. D **99,** 121302 (2019).

[22] G.-B. Zhao *et al.*, Nat. Astron. **1,** 627 (2017).

[23] Y. Zhang, H. Zhang, D. Wang, Y. Qi, Y. Wang, and G.-B. Zhao, Res. Astron. Astrophys. **17,** 050 (2017).

[24] E. Di Valentino, A. Melchiorri, E. V. Linder, and J. Silk, Phys. Rev. D **96,** 023523 (2017).

[25] J. Sola Peracaula, A. Gomez-Valent, and J. d. C. Perez, Phys. Dark Universe **25,** 100311 (2019).

[26] E. Di Valentino, R. Z. Ferreira, L. Visinelli, and U. Danielsson, Phys. Dark Universe **26,** 100385 (2019).

[27] P. Agrawal, G. Obied, and C. Vafa, arXiv:1906.08261.

[28] K. Dutta *et al.*, arXiv:1808.06623.

[29] L. Visinelli, S. Vagnozzi, and U. Danielsson, Symmetry **11,** 1035 (2019).

[30] X. Li and A. Shafieloo, arXiv:1906.08275.

[31] S. Adhikari and D. Huterer, arXiv:1905.02278.

[32] H. Desmond, B. Jain, and J. Sakstein, Phys. Rev. D **100,** 043537 (2019).

[33] L. Kazantzidis and L. Perivolaropoulos, arXiv:1907.03176.

[34] W. L. Freedman *et al.*, Astrophys. J. **882,** 34 (2019).

[35] W. Yuan, A. G. Riess, L. M. Macri, S. Casertano, and D. Scolnic, arXiv:1908.00993.

[36] M. Chevallier and D. Polarski, Int. J. Mod. Phys. D **10,** 213 (2001).

[37] E. V. Linder, Phys. Rev. Lett. **90,** 091301 (2003).

[38] T. D. Saini, S. Raychaudhury, V. Sahni, and A. A. Starobinsky, Phys. Rev. Lett. **85,** 1162 (2000).

[39] F. Beutler, C. Blake, M. Colless, D. H. Jones, L. Staveley-Smith, L. Campbell, Q. Parker, W. Saunders, and F. Watson, Mon. Not. R. Astron. Soc. **416,** 3017 (2011).

[40] A. J. Ross, L. Samushia, C. Howlett, W. J. Percival, A. Burden, and M. Manera, Mon. Not. R. Astron. Soc. **449,** 835 (2015).

[41] M. Ata *et al.*, Mon. Not. R. Astron. Soc. **473,** 4773 (2018).

[42] S. Alam *et al.* (BOSS Collaboration), Mon. Not. R. Astron. Soc. **470,** 2617 (2017).

[43] H. du Mas des Bourboux *et al.*, Astron. Astrophys. **608,** A130 (2017).

[44] M. J. Reid, J. A. Braatz, J. J. Condon, L. J. Greenhill, C. Henkel, and K. Y. Lo, Astrophys. J. **695,** 287 (2009).

[45] M. J. Reid, J. A. Braatz, J. J. Condon, K. Y. Lo, C. Y. Kuo, C. M. V. Impellizzeri, and C. Henkel, Astrophys. J. **767,** 154 (2013).

[46] C. Kuo, J. A. Braatz, M. J. Reid, F. K. Y. Lo, J. J. Condon, C. M. V. Impellizzeri, and C. Henkel, Astrophys. J. **767,** 155 (2013).

[47] F. Gao, J. A. Braatz, M. J. Reid, K. Y. Lo, J. J. Condon, C. Henkel, C. Y. Kuo, C. M. V. Impellizzeri, D. W. Pesce, and W. Zhao, Astrophys. J. **817,** 128 (2016).

[48] M. J. Reid, D. W. Pesce, and A. G. Riess, arXiv: 1908.05625.

[49] V. Bonvin *et al.*, Mon. Not. R. Astron. Soc. **465,** 4914 (2017).

[50] A. Gómez-Valent and L. Amendola, J. Cosmol. Astropart. Phys. 04 (2018) 051.

[51] S. Nesseris, G. Pantazis, and L. Perivolaropoulos, Phys. Rev. D **96,** 023542 (2017).

[52] L. Kazantzidis and L. Perivolaropoulos, Phys. Rev. D **97,** 103503 (2018).

[53] D. Foreman-Mackey, D. W. Hogg, D. Lang, and J. Goodman, Publ. Astron. Soc. Pac. **125,** 306 (2013).

[54] V. de Sainte Agathe *et al.*, Astron. Astrophys. **629,** A85 (2019).

[55] H. Hildebrandt *et al.*, arXiv:1812.06076.

[56] S. Joudaki *et al.*, arXiv:1906.09262.

[57] K. Liao, A. Shafieloo, R. E. Keeley, and E. V. Linder, arXiv:1908.04967.